

# Living Biointerfaces for the Maintenance of Mesenchymal Stem Cell Phenotypes

Michaela Petaroudi, Aleixandre Rodrigo-Navarro, Oana Dobre, Matthew J. Dalby, and Manuel Salmeron-Sanchez\*

Living interfaces are established as a novel class of active materials that aim to provide an alternative to traditional static cell culture methods by enabling users to accurately control cell behaviour in a precise, dynamic, and reliable system-internal manner. To this day, the only reported biointerface has been a coculture between a biofilm of nonpathogenic genetically engineered bacteria and mammalian cells, where the recombinant proteins produced by the bacteria directly influence cell behaviour. In this work, a biointerface is presented between *Lactococcus lactis* (*L. lactis*) and human mesenchymal stem cells (hMSCs). *L. lactis* have been engineered to produce human C-X-C motif chemokine ligand 12, thrombopoietin, vascular cell adhesion protein 1, and the 7th–10th type III domains of human fibronectin, with the aim of recreating the native bone marrow conditions *ex vivo*. This active microenvironment has been shown to maintain key hMSC stemness markers, preventing their osteogenic and adipogenic differentiation, and maintaining high stem cell viability and physiological cell-to-substrate adhesion dynamics. This work presents proof of concept data that hMSC stemness can be regulated by living materials, using a system based on the symbiotic interaction between different engineered bacteria and mammalian cells.

of exploiting the material properties of biocompatible polymers and scaffolds to create and mimic a microenvironment for natural tissue growth could be used in a variety of clinical settings such as transplant development or organ regeneration.<sup>[3–5]</sup>

Human mesenchymal stem cells (hMSCs),<sup>[6,7]</sup> also known as multipotent mesenchymal stromal cells<sup>[6]</sup> are a key player in tissue engineering because of their remarkable potential to differentiate into a variety of cell types when stimulated with the appropriate biochemical, physical and mechanical cues. This has placed MSCs in the spotlight of regenerative medicine research and has created the need to develop strategies in order to control the cells' fate in a precise and reproducible manner.<sup>[8]</sup> Despite the wide variety of literature reporting hMSC differentiation studies, efforts to precisely control the differentiation of these cells have been impaired due to the complexity of the proposed systems.<sup>[9]</sup>

Aside from the importance of the control of hMSC differentiation, recent research has started to shift toward exploring ways of maintaining the naïve, stem-like phenotype of the cells. The rapid loss of the innate self-renewal and multilineage differentiation potential of hMSCs with every cell division has highlighted the need for the establishment of new methods of preserving hMSC multipotency after lengthy cell cultures and expansions. Different approaches aiming to maintain the stemness of hMSCs have focused on a variety of intrinsic and extrinsic parameters that could be manipulated to regulate the cells' fate.<sup>[10]</sup> The regulation of nuclear receptors,<sup>[11]</sup> microRNAs,<sup>[12]</sup> as well as signaling pathways has been extensively studied for the maintenance of stemness in hMSCs. Furthermore, culture conditions, such as spatial confinement,<sup>[13]</sup> substrate stiffness<sup>[14]</sup> elasticity<sup>[15]</sup> and nanotopography,<sup>[16,17]</sup> as well as hypoxia<sup>[18]</sup> have been examined as a potential mechanism to direct hMSC fate.

Recently, living materials have been reported as a novel, simple and tuneable way of controlling stem cell fate and have been recently explored due to their promising potential for therapeutic applications.<sup>[19–22]</sup> The active nature of this new class of biomaterials has the potential to provide a closer representation of natural systems and cell niches, as it can be used to provide

## 1. Introduction

The growing demand for novel and efficient therapeutic methods to treat complex clinical conditions has created the need for new approaches in regenerative medicine.<sup>[1]</sup> Tissue engineering is a field of growing scientific interest due to its interdisciplinary approach of combining the physical and biological characteristics of human tissues with the principles of engineering and materials science.<sup>[2]</sup> The possibility

M. Petaroudi, A. Rodrigo-Navarro, O. Dobre, M. J. Dalby, M. Salmeron-Sanchez  
Centre for the Cellular Microenvironment  
University of Glasgow  
Glasgow G12 8LT, UK  
E-mail: manuel.salmeron-sanchez@glasgow.ac.uk

 The ORCID identification number(s) for the author(s) of this article can be found under <https://doi.org/10.1002/adfm.202203352>.

© 2022 The Authors. Advanced Functional Materials published by Wiley-VCH GmbH. This is an open access article under the terms of the Creative Commons Attribution License, which permits use, distribution and reproduction in any medium, provided the original work is properly cited.

DOI: 10.1002/adfm.202203352

cultured cells with signals of interest in a regulated, more physiologically relevant way. The ability of bacteria to be used as a biologically active substrate for cell culture and engineering and the variety of tools available for recombinant protein engineering and expression by such a biointerface, open a wide range of possibilities for the simulation of natural cellular microenvironments, without the use of artificial, inert materials, or traditional static culture conditions. Light-controlled living materials,<sup>[19,20]</sup> bacterial ligand display and secretory protein expression,<sup>[21,22]</sup> as well as light-controlled mammalian cell response on the light-regulated biointerface<sup>[23]</sup> have been previously reported in the literature. However, these efforts have been focusing on the active material side of the interface and even though they successfully report innovative approaches in active materials systems, they rarely report the effect of their system on human stem cells.

Genetically engineered biofilms of the nonpathogenic bacteria *L. lactis*, have been reported to induce the differentiation of murine C2C12 myoblasts into myotubes, upon extracellular presentation of the recombinant fibronectin fragment FN III<sub>7-10</sub> (hereinafter FN).<sup>[24]</sup> Bacteria-based materials have also been shown to successfully drive osteogenic differentiation of human MSCs by recombinantly produced and secreted bone morphogenetic protein-2 (BMP-2) and have been established as a symbiotic interface between eukaryotic and prokaryotic cells.<sup>[10,25]</sup> Here, we develop a new range of bacteria-based materials to

tackle another aspect of stem cell fate control, the maintenance of a naïve, stem-like phenotype in human bone marrow (BM) MSCs. To achieve this, we have genetically engineered the *L. lactis* NZ9020 strain to produce CXCL12, TPO, VCAM1, and FN. The selected cytokines are widely recognized as important regulators of the bone marrow niche, where MSCs are maintained in a naïve, highly proliferative state, and have been associated with MSC survival and proliferation in vitro. Hence, the mentioned signaling molecules have been selected to maintain the MSCs in an undifferentiated way, similar to their BM phenotype, and encourage their proliferation in vitro, and have been used in combinations with the view to create a cell culture system resembling the bone marrow, where the cytokines are constantly and jointly expressed. We have assessed the impact of biofilms made up of the above cytokine-expressing bacterial populations on the viability, adhesion and spreading, migration, as well as phenotype maintenance of hMSCs seeded directly on the biofilms and cultured for up to 14 d.

## 2. Results

### 2.1. Recombinant Protein Expression in *L. lactis*

Figure 1A represents a schematic overview of the system. An *L. lactis* biofilm was allowed to develop as a monolayer on

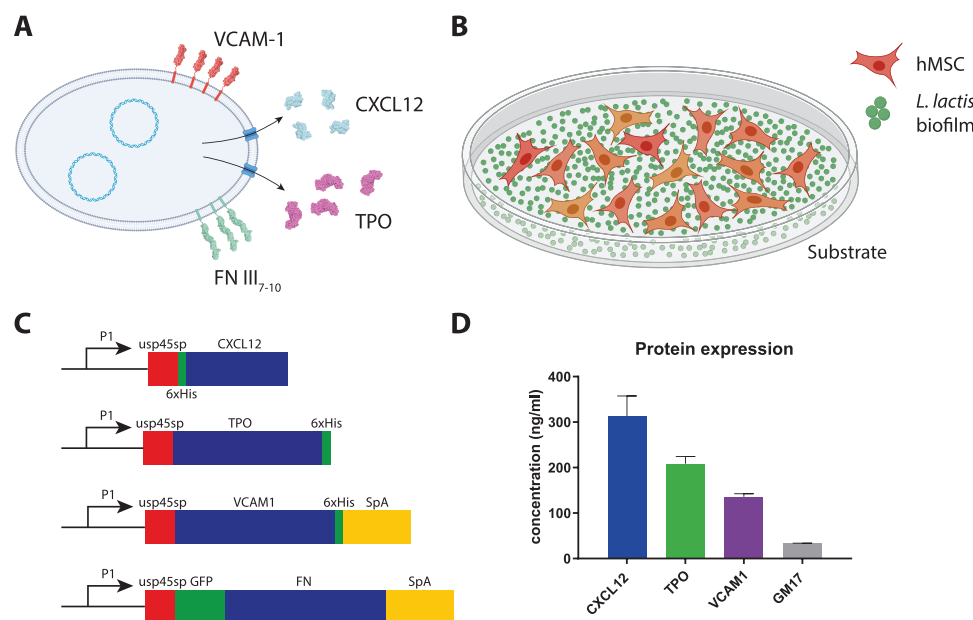


**Figure 1.** A) Schematic overview of the system. A glass substrate was treated with (3-aminopropyl) triethoxysilane (APTES) or Sigmacote to increase surface hydrophobicity and allow the development of more stable and denser biofilms. Then, an *L. lactis* biofilm was developed on the silanized surface. Human bone marrow-derived mesenchymal stem cells were cocultured with the *L. lactis* biofilm for variable amounts of time. B) *L. lactis* NZ9020 were electrotransformed with plasmids carrying ORFs for human CXCL12, TPO, VCAM1, and FN III<sub>7-10</sub>. Each bacterial population was engineered to produce a single recombinant protein. TPO and CXCL12 were secreted extracellularly using the lactococcal *usp45* secretion peptide. VCAM1 and FN III<sub>7-10</sub> were cloned upstream the *S. aureus* protein A domain that contains the LPETG motif, that allows for a covalent linking to the peptidoglycan cell wall of the bacteria, effectively displaying the proteins in the bacterial cell wall. C) Schematic of the plasmid constructs. All proteins were placed under the control of the strong constitutive lactococcal P1 promoter followed by the phage T7 gene 10' 5'-UTR and RBS. *Usp45sp* was used as a secretion signal, followed by the gene of interest and the C-terminal end (residues 268–457) of *S. aureus* protein A for cell wall binding. D) Protein expression levels were measured using a competitive ELISA against the 6xHis tag present in the CXCL12, TPO, and VCAM1 plasmids. M17, the *L. lactis* culture medium, supplemented with 0.5% glucose, was used as a negative control. FN was not included in this graph because its expression level was determined in a previous work—fully developed biofilms expressed FN at a concentration of 6.32 ng cm<sup>-2</sup>.<sup>[10]</sup>

sterile silanized borosilicate glass coverslips and hMSCs were cultured on top of the bacterial monolayer. Previous work has shown that the hMSCs interact and adhere to the biofilm through focal adhesions to the FN fragment expressed in the bacterial cell wall.<sup>[10,25]</sup> Here, *L. lactis* NZ9020 has been genetically engineered to produce secreted recombinant CXCL12 and TPO, as well as the extracellular domain of the VCAM1 and FN adhesion peptides. All proteins have been placed under the control of the strong P1 lactococcal promoter<sup>[26]</sup> and fused to the signal peptide of the *usp45* lactococcal protein.<sup>[27]</sup> For the extracellular presentation of the VCAM1 and FN fragments, the *S. aureus* protein A (SpA), that contains the LPETG motif, was fused to the C-terminus of the proteins, allowing for covalent crosslinking of the protein fragment to the outer peptidoglycan layer of *L. lactis*.<sup>[28]</sup> Only the extracellular domain of VCAM1 was chosen for expression in *L. lactis* since it contains the protein's active site, including the integrin  $\alpha_4\beta_1$  binding site.<sup>[29]</sup> Similarly, the FN fragment has been shown to be biologically active in a variety of studies.<sup>[30]</sup> For easier protein characterization and quantification, a hexahistidine (6xHis) tag was added to either the N or C-terminus of the proteins.

Protein expression was quantified from either the supernatant of 10 ml bacterial cultures grown for 16 h for secreted proteins, or after pelleting and lysis of the bacterial cells followed by a competitive ELISA against the 6xHis tag (Figure 1B). Despite the use of the same promoter and RBS, all four recombinant proteins were expressed at different rates. To explain and evaluate the effect of protein production on the growth rate of each bacterial population, we monitored the growth of the bacterial populations over the course of 1000 min. All strains showed different doubling time and growth constant (k) (Figure S1, Supporting Information), suggesting that the size of the expressed protein imposes some metabolic burden in the bacteria, has some impact on its doubling time and concomitantly may affect the amount of expressed protein. The strains expressing CXCL12, TPO and the control showed similar growth kinetics, while expression of FN and VCAM1 seemed to impose an additional metabolic burden on *L. lactis* cells. However, the differences were small enough to allow for the coculture of different strains in the same biofilm. Since the different populations follow similar growth trends for the first 12–16 h of culture, which is the normal overnight biofilm formation time, we can suggest that a biofilm formed by different populations would feature all populations, with neither of them being overrun by the faster growing strains. When established into the biofilm, the bacterial growth would slow down significantly and therefore, the bacteria that initially populate the biofilm would remain in it. With no intra-population competition in the same biofilm bacteria, we suggest that the bacterial populations can be used in combinations without one outcompeting the others.

The bioactivity of recombinant FN expressed in *L. lactis* has been previously assessed.<sup>[22]</sup> In this work, we evaluated the biological activity of the CXCL12 and TPO expressed by the biofilms by conducting motility studies on hMSC and viability/proliferation studies on human erythroleukemic TF-1 cells (Figure S6, Supporting Information). In particular, the ability of CXCL12 to induce increased hMSC motility has been supported and reviewed in detail,<sup>[34,35]</sup> and identified as a requirement for

hMSC mobilization and migration in vitro.<sup>[36,37]</sup> Our results suggest a significantly increased motility speed in the hMSCs stimulated by both the commercial and *L. lactis*-expressed CXCL12, compared to both the media conditioned by the EMPTY (control, no secreted recombinant proteins) bacteria and to the control media (Figure S6A,B, Supporting Information). At the same time, no statistically significant differences were recorded in the hMSCs cell speed displayed in response to commercial and *L. lactis*-expressed CXCL12. Additionally, the biological activity of the TPO expressed by *L. lactis* was assessed by its effect on TF-1, a cell line that has been identified to show a proliferative response to TPO.<sup>[38]</sup> The data shows that no statistically significant differences were observed between the proliferative behavior of TF-1 cells cultured in media supplemented with commercially sourced and *L. lactis*-expressed TPO (Figure S6C, Supporting Information). Given the TF1 cell line dependence on TPO, the cells cultured in the control media, without TPO supplementation, showed lowered proliferation rates during the first 3 d of culture, and the viability dropped after that time point.

## 2.2. Characterization of Living Biointerfaces

In previous work, biofilms were developed on hydrophilic borosilicate glass coverslips, and even though the bacteria remained viable,<sup>[24]</sup> the weak adhesion of the biofilm to the surface proved insufficient to support longer term cultures. To provide a stronger attachment than the weak van der Waals and Lewis acid-base forces that govern the interaction between a biofilm and its substrate, we tested different coatings. In this work, we used the *L. lactis* strain NZ9020, which bears a knockout of the lactate dehydrogenase *ldhA* and *ldhB* genes,<sup>[36]</sup> and is more suited to biomedical applications due to the subsequent reduction in lactic acid production and the subsequent acidification of the cell culture media. Similarly to NZ9000, NZ9020 shows a strong negative net surface charge in physiological conditions.<sup>[37]</sup> Since hydrophobicity has been shown to play a role in bacterial attachment to surfaces,<sup>[38]</sup> we tested different silanes as coatings for long term biofilm culture on glass coverslips to reduce the surface zeta potential and increase the interaction strength with the bacterial surfaces. We selected (3-aminopropyl) triethoxysilane (APTES) and Sigmacote, two silanes extensively used as a surface coating to support stem cell cultures<sup>[39,40]</sup> in order to achieve stronger, long term adhesion due to the electrostatic interaction between the bacteria and the treated glass surface.

Tetracycline (TC) is a bacteriostatic antibiotic that when used at 10  $\mu\text{g mL}^{-1}$  inhibits bacterial protein synthesis through blocking the attachment of the charged aminoacyl tRNA to the A-site of the bacterial ribosome,<sup>[41]</sup> allowing to keep the bacteria in a reduced metabolic state and slowing down its proliferative potential and preventing the accumulation of lactic acid in the culture medium. Sulfamethoxazole (10  $\mu\text{g mL}^{-1}$ ) and erythromycin (5  $\mu\text{g mL}^{-1}$ ) were also used to further control the proliferative rate of *L. lactis* in the cocultures and in the case of erythromycin, to exert a selective pressure on the *ldhA* and *ldhB* phenotype of *L. lactis* NZ9020. *L. lactis* biofilms were produced in M17 medium supplemented with 0.5% glucose and 10  $\mu\text{g mL}^{-1}$  chloramphenicol (GM17C) and after the biofilm was

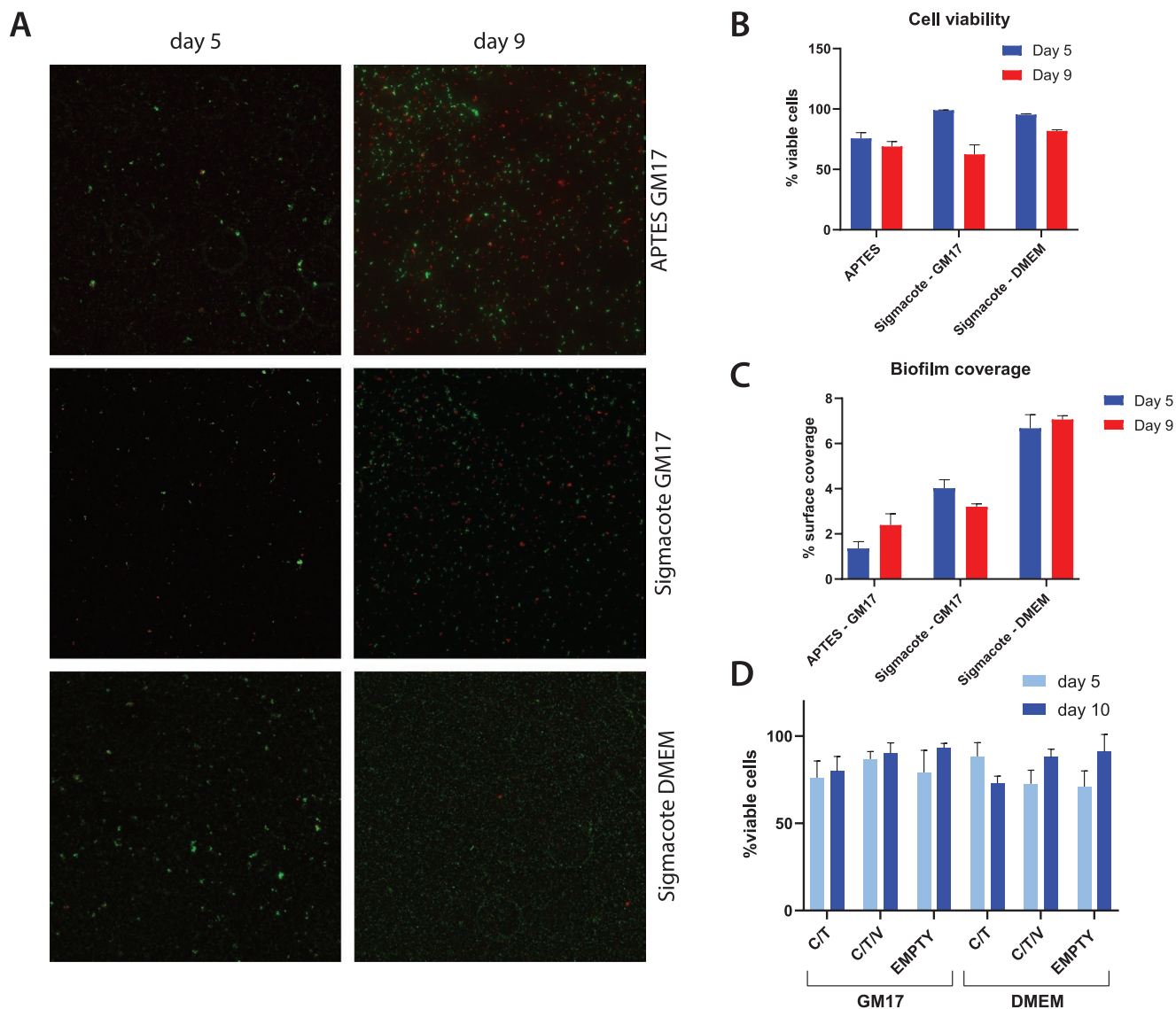


**Figure 2.** Biofilm characterization. A,B) Viability of the biofilms used in the coculture experiments, produced by combining CXCL12 (C), TPO (T), and VCAM1 (V) at different ratios and the control strain, were determined after 5 or 10 d using the FilmTracer viability kit. Viability values do not show a statistically significant difference ( $p \geq 0.05$ ) between the different strains and time points. Panel (A) shows representative images showing biofilms' viability on the different tested surfaces and culture media. In this case, the C/T biofilm is depicted and GM17 and DMEM were used to compare the different culture conditions and their effect on the bacterial biofilm. No statistically significant differences were found ( $p \geq 0.05$ ) between the different time points or conditions. C) Biofilm area density, here shown *L. lactis*-CXCL12, as in percentage of area covered by the bacterial biofilm, was determined for the same conditions used in panels (B) and (C) at the same time points. Surfaces treated with Sigmacote kept a higher biofilm density compared to APTES, and DMEM showed the higher values. Panel (D) shows biofilms' viability on the different tested surfaces and culture media. In this case, GM17 and DMEM were used to compare the different culture conditions and their effect on the bacterial biofilm. No statistically significant differences were found ( $p \geq 0.05$ ) between the different time points or conditions. We acknowledge a reduced viability value on days 5 and 9 for GM17 in Sigmacote but no statistically significant difference was found with the available data and this trend could be attributed to leaving the *L. lactis* cells in GM17, which reaches a pH around  $\approx 5$  and has a detrimental effect on cell viability. Longer term cultures have been done in DMEM at a physiological pH of 7.4, which has a less detrimental effect as seen in the graph. A representative phase contrast image of a biofilm cultured in Sigmacote-DMEM for 9 d is shown in the image on the right. Results were obtained by counting the number of live bacteria per field of view, in three biological replicates, and three individual experiments. The displayed data represent mean  $\pm$  S.E.M. and was analyzed with a Student's t-test.

developed, the growth medium was changed to DMEM plus tetracycline, sulfamethoxazole and erythromycin at the same concentrations to prevent bacterial proliferation and its associated medium acidification.

*L. lactis* has been shown to form stable biofilms that can remain viable up to 10 d (Figure 2A,B). Data suggest no

significant reduction in biofilm viability measured after 5 and 10 d in culture, while also showing that the high viability observed is maintained both in GM17 and DMEM. This evidence supports our claim that the biofilms can be cultured in a variety of different media, supporting different cocultures with human stem cells. Furthermore, in efforts to increase

biofilm stability and ensure a strong adhesion to the coverslip, we measured bacterial viability cultured in the presence of this antibiotic mix in both Sigmacote and APTES-treated glass surfaces. The viability of the biofilm did not display any statistical differences between APTES and Sigmacote after 9 d of culture (Figure 2C), and despite the slight reduction in the number of viable cells between the 5th and 9th day, the biofilm retained high viability values (above 75%) after 9 d of culture in DMEM. However, the biofilms cultured on Sigmacote-treated coverslips showed increased coverage compared to the ones cultured on APTES-treated surfaces (Figure 2D), suggesting that Sigmacote is a more suitable coating for use in further experiments. Biofilm surface coverage was measured after 5 and 9 d in glass coverslips treated with APTES and Sigmacote, that has been shown to induce a higher surface coverage compared to APTES (Figure 2C) and was therefore selected as a coverslip coating for further long-term cultures. Despite the low surface coverage, we suggest that the constitutive nature of the production of the recombinant proteins could be used to replace the traditional method of adding high levels of cytokines to the cell culture media and would provide a closer representation of natural stem cell niches, where the cells are constantly receiving a variety of chemical and adhesion stimuli from other components of their niche. A lower level of surface coverage would also be preferable for our system, as a larger number of bacteria could overflow the media with recombinant proteins and a higher level of metabolic end products, which could have negative effects to both stem cell viability and induce the development of undesirable cell phenotypes.

### 2.3. hMSC Adhesion and Viability on the Biofilms

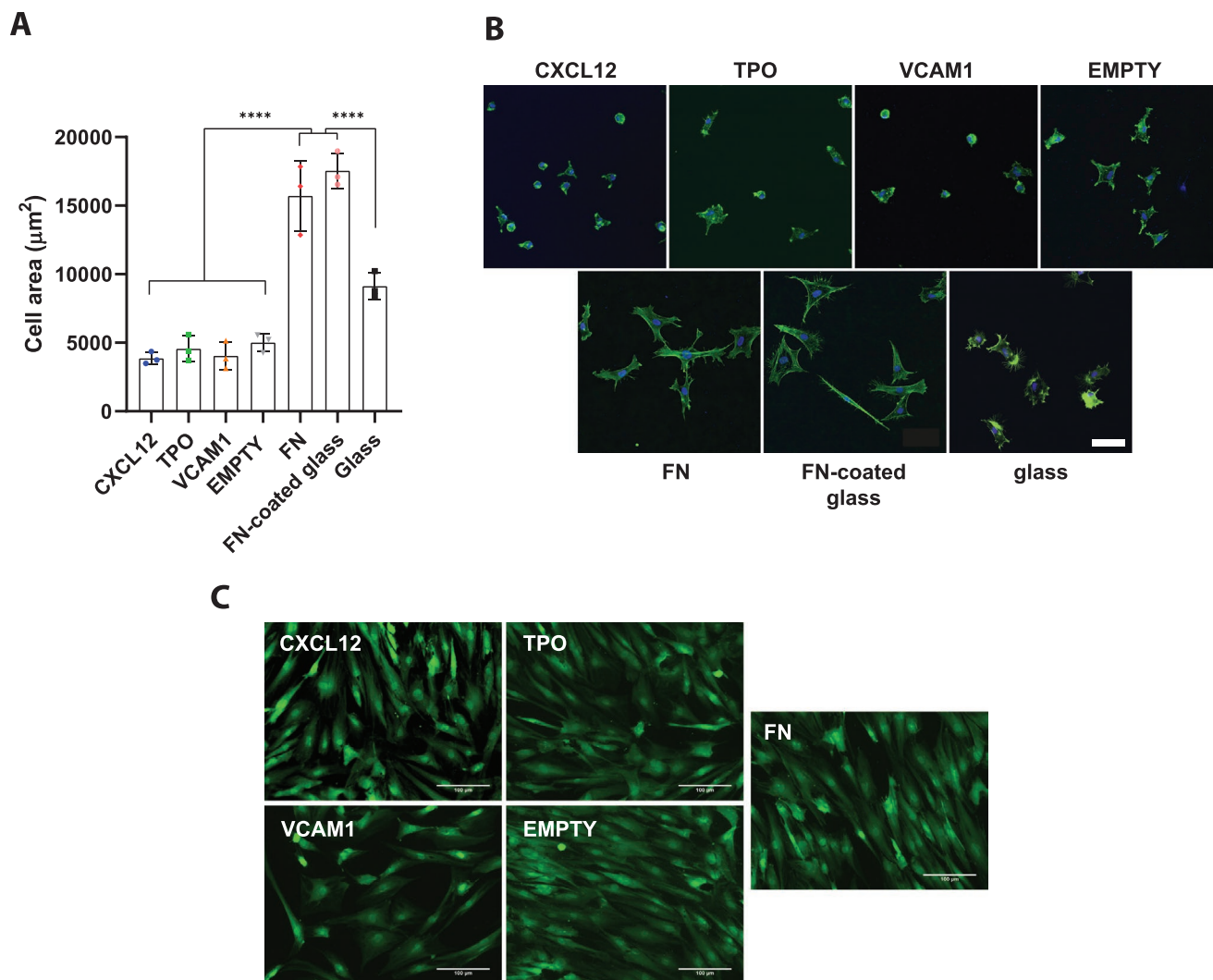
Human mesenchymal stem cells (hMSCs) adhesion and morphology on the *L. lactis*-based biointerfaces was assessed by actin staining. The cells were cultured for 3 h in DMEM supplemented with tetracycline, sulfamethoxazole, erythromycin and without FBS to prevent deposition of other serum proteins that might hide the effect of bacteria. Cell area was determined using image analysis of the actin staining. The hMSCs showed adhesion and spreading, with focal adhesion development (Figure S2, Supporting Information). Interestingly, no statistically significant differences were observed between the frequency or area of focal adhesions developed by the hMSCs on the different biofilms (Figure S2A,B, Supporting Information), suggesting that the stem cells interact in a similar way with the biofilms, regardless of the recombinant protein produced by the bacteria. In contrast, actin staining shows that the cells displayed different morphologies depending on the type of biofilm they were cultured on (Figure 3A,B). hMSCs cultured on CXCL12, TPO, VCAM1, and EMPTY biofilms displayed a significantly smaller area compared to the cells grown on the FN-expressing biofilm as well as the two glass coverslip controls. The area of the cells cultured on the FN-expressing biofilm appeared statistically comparable to the area of hMSCs cultured on the FN-coated glass coverslip, while in both cases, the cells acquired a more spread phenotype compared to the glass coverslip (Figure 3A).

Image analysis of the actin staining has shown that hMSC area appears statistically comparable between the bacterial populations expressing CXCL12, TPO and VCAM1, as well as the EMPTY biofilm, where they appear to adhere to the bacteria but retain a small, round-like morphology. In contrast, hMSCs cultured on the FN-expressing biofilms display a much more spread phenotype, featuring larger, more elongated cells, similar to the one observed in the fibronectin-coated substrate and glass coverslip (Figure 3B).

Finally, we show that the viability of the human cells remains unaffected by the biofilm after 3 and 5 d in culture. We failed to detect any dead cells in any of the tested time points or conditions (Figure 4C), proving that mammalian cells can be safely cocultured with *L. lactis* NZ9020. This observation further underlines the ability of *L. lactis* to be cocultured with hMSCs and agrees with the existing literature on its potential to be used in a variety of biotechnological and biomedical applications.<sup>[42,43]</sup> In total, we noted that since it is known that the hMSCs cultured on the biofilms start secreting their own extracellular matrix (ECM) after a day, the presence of ECM proteins such as fibronectin results in a more spread phenotype as it is evident from the live/dead assay, compared to the actin staining after 3 h of culture.

### 2.4. hMSC Motility on Biofilms

Inspired by the constant state of flux and remodeling that characterizes native stem cell niches,<sup>[44,45]</sup> we aimed to evaluate the way hMSCs move and explore their surroundings in our system. To study cell movement in physiologically relevant conditions, we tailored our experimental setup to resemble the architecture of the BM. To mimic the 3D structure of the niche, we tracked hMSC trajectories on different *L. lactis* biofilms, with and without the presence of a hydrogel, bearing stiffness and porosity within the range found in human BM.<sup>[46–48]</sup> In particular, we engineered our hydrogels with a Young's modulus of 3 kPa, that falls in the range of natural bone marrow, ranging from 0.5–5 kPa in the perivascular and up to 40 kPa in the endosteal niche. Initially, we examined whether there is a difference between hMSC movement in 2D and 2.5D, by tracking cells seeded directly on the biofilms (2D) and comparing them to cells seeded in a monolayer between the biofilms and a hydrogel (2.5D). Figure S4 (Supporting Information) depicts the trajectories followed by the cells at different time points and in different culture conditions. Some differences are found in the speed of MSCs at day 1 on the different biofilms in the absence of hydrogels, which disappear after 3 d of culture. However, already at 24 h of tracking the cells displayed a significant difference between the range and speed of motion exhibited by the hMSCs in the presence of a hydrogel compared to its absence (Figure 4A). Cells seeded in 2D were highly motile and appeared to actively explore their surroundings, following large trajectories. In contrast, the presence of the hydrogel appeared to significantly restrict cell movement, resulting in less active motile cells that largely remained attached to their starting point. The same trend was observed after analysis of cell speed, with much higher average cell speeds measured in 2D compared to 2.5D.



**Figure 3.** A) Cell area of hMSCs cultured on biofilms expressing CXCL12, TPO, VCAM1, and FN (note this is FN IIII7–10) was measured by image analysis and was compared to an EMPTY biofilm as well as hMSCs grown on FN-coated and bare glass coverslips. Cells grown on CXCL12, TPO, VCAM1, and EMPTY biofilms were significantly smaller in size compared to cells grown on the FN-expressing biofilm and the two glass coverslip conditions (A minimum of 15 cells per biological replicate and per condition were analyzed) after a one-way nonparametric ANOVA with Kruskal-Wallis post hoc test ( $\alpha = 0.05$ ,  $**** p < 0.001$ ). Data presented as mean  $\pm$  SD. B) Actin-stained hMSCs cultured on the different biofilms. C) hMSC viability on *L. lactis* biofilms. Representative images of the live/dead assay are shown for each condition. Viable hMSCs are displayed in green, while no nonviable hMSCs were recorded (red channel). This might be due to dead cells being washed away to prepare the staining, a known limitation of this technique. hMSC viability of cells cultured on CXCL12, TPO, FN, VCAM1 for 3 and 5 d was determined with a mammalian viability kit (ThermoFisher). No nonviable (red-stained) cells were found. Thus, we infer that there were only a limited number of nonviable cells across the different tested conditions. ANOVA; analysis of variance, SD; standard deviation.

Following this observation, we aimed to examine the effect of hydrogel degradability on cell movement. In a similar experiment, we seeded hMSCs on the *L. lactis* biofilms and tracked cell movement in the presence of a nondegradable and a degradable polyethylene glycol (PEG) hydrogel. To provide a close BM analogue, we fabricated protease-degradable hydrogels, using the crosslinking peptide GCRDVPMSMRG-GDRCG (VPM),<sup>[49]</sup> which is rapidly cleaved by matrix metalloproteinases 1 and 2 (MMP-1 and MMP-2).<sup>[53]</sup> The degradable hydrogels were synthesized with a 1:1 PEG:VPM ratio, while the nondegradable hydrogels consisted of 100% PEG. To allow enough time for the cells to degrade and remodel their 3D environment, we tracked cell movements at days 3, 5, and 7,

after seeding. Analysis of the cell trajectories and average cell speed suggested a significant difference between the cells cultured in contact with the degradable and nondegradable hydrogels (Figure 4 B–D). The difference was more pronounced on days 3 and 7, with the hMSCs cultured in the presence of the PEG-VPM hydrogel moving at an observably higher speed compared to the nondegradable condition. While most differences in cell movement appear to have settled by day 5, we again observed a significant change at day 7, with similar cell movement trends as observed in day 3. The collective observation that hMSCs cultured in the presence of degradable hydrogels are more active in exploring their surroundings and move at a higher speed compared to cells cultured in nondegradable

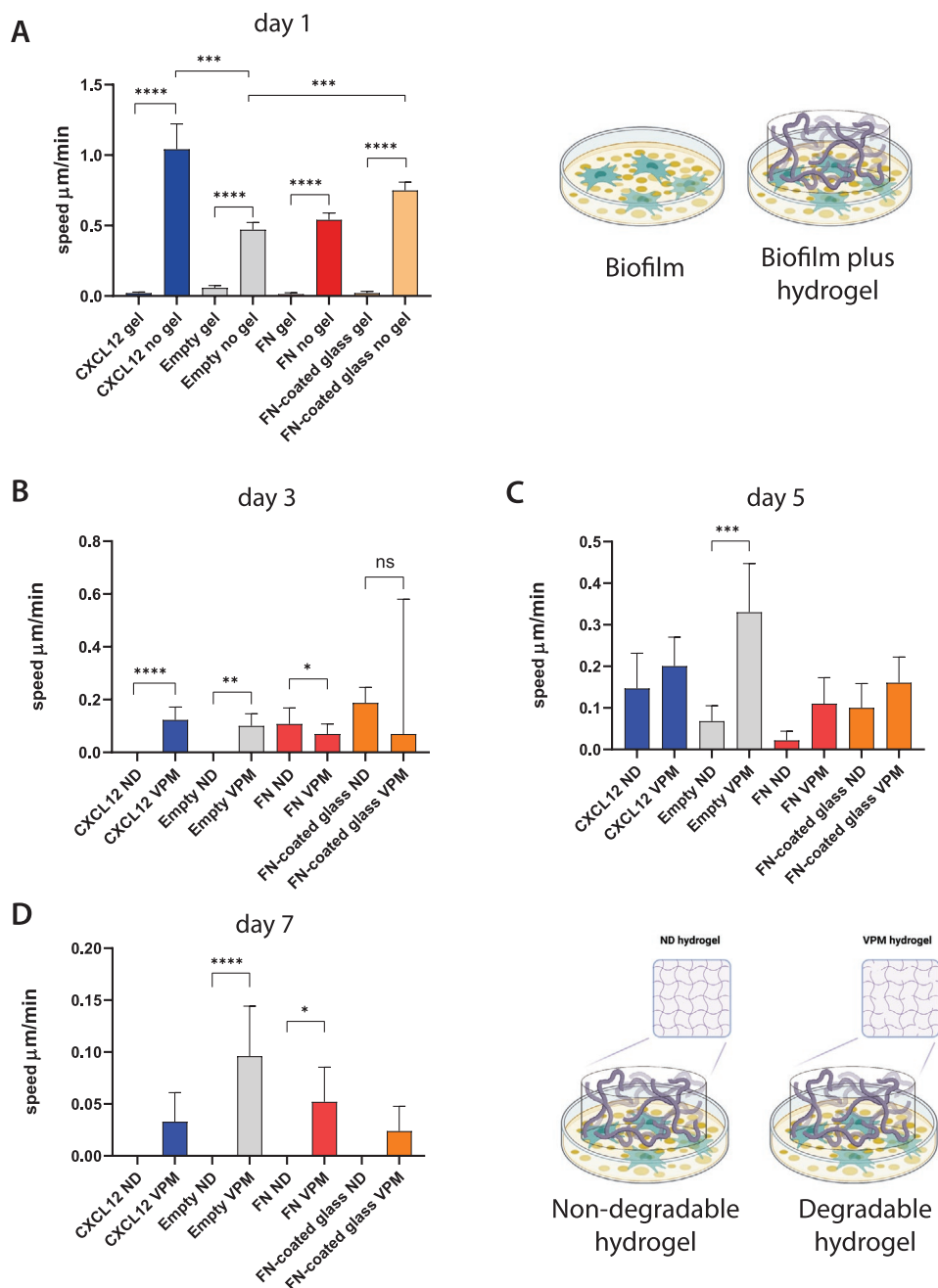


**Figure 4.** Motility experiments and cell speed and trajectories. Human MSCs were seeded on *L. lactis* biofilms in either 2D or 2.5D conditions and were tracked at different time points. A) The cells were initially tracked for 24 h, with 5 min intervals after an initial overnight incubation to allow cells to adhere to the substrate. The average speed by cell was recorded and comparisons were drawn between the cells incubated with and without the presence of a hydrogel and between the different biofilm conditions. B–D) Cells were incubated on top of *L. lactis* biofilms in the presence of either a nondegradable (PEG) or a degradable (VPM) hydrogel. Cell speed was measured after tracking for 1 h with 2 min intervals on days 3, 5, and 7 of the cocultures. Data presented as mean  $\pm$  SD and analyzed with ANOVA with a Tukey post hoc test. A minimum of 15 cells were measured per condition, in three independent experiments. Significance levels are \* $p < 0.05$ , \*\* $p < 0.01$ , \*\*\* $p < 0.001$ , \*\*\*\* $p < 0.0001$ ; ANOVA, analysis of variance; SD, standard deviation.

2.5D conditions is further supported by mean displacement analysis data, which suggests a larger area explored by hMSCs cultured in the degradable hydrogel conditions. Notably, the higher cell speeds recorded on day 5 compared to day 3, especially in the degradable hydrogels shows the ability of MSCs to actively interact with their microenvironment, and initiate

the degradation of the hydrogels, resulting in their ability to more freely migrate and explore their surroundings by day 5. The subsequent drop in migration speed on day 7 could be attributed to changes in cell proliferation, which could perhaps result in a decrease of cell movement in order to prioritize cell division.

## 2.5. HMSC Phenotyping

To evaluate the effect of the different bacteria-based interfaces, expressing different recombinant proteins on hMSC fate, we performed 14 d coculture experiments and followed by in-cell Western (ICW) analysis of phenotype. The MSCs were cultured on *L. lactis* populations expressing either single recombinant proteins or combinations of different cytokines. This experimental setup aims to both assess the effect of each cytokine on the maintenance of the stem cell phenotype, and to investigate our hypothesis that combinations of expressed cytokines by the biofilms may provide a closer representation of the native BM stimuli that the MSCs experience in their niche, which may in turn induce MSC maintenance. We selected the osteogenic markers osteopontin (OPN)<sup>[51,52]</sup> and osterix (OSX)<sup>[52]</sup> and the stemness markers nestin,<sup>[53]</sup> Stro1,<sup>[54,55]</sup> and Activated Leukocyte Cell Adhesion Molecule (ALCAM)<sup>[56]</sup> that have been widely used in the literature to assess hMSC phenotype. The results were normalized against the housekeeping protein  $\beta$ -actin, commonly used to obtain reliable and reproducible quantitative results in real-time quantitative PCR, Western blot and ICW analysis.<sup>[57]</sup>

Figure 5 represents the ICW results for the hMSC phenotype assessment after 14 d of culture on different biofilms. To assess the maintenance of a naïve hMSC phenotype, we selected Stro1, nestin and ALCAM. All three markers have been extensively used in the literature to select for hMSCs with an immature phenotype.<sup>[58,59]</sup> All stemness markers (ALCAM, nestin and Stro1) were expressed after 14 d in all conditions (Figure 5A–C). Despite the obvious overexpression of ALCAM and Stro1 of the hMSCs cultured on biofilms consisting of mixed *L. lactis* populations expressing TPO/FN/VCAM1 (Figure S5A,C, Supporting Information), the difference is not significant compared to the hMSC control. Furthermore, nestin expression was comparable between the hMSCs cultured on all biofilms and the control (Figure 5B). Together, these results suggest that hMSCs cultured on recombinant *L. lactis* biofilms has the potential to maintain a stem-like phenotype on the cells in a similar way to naïve hMSCs cultured for one day (hMSC control).

Staining for osteogenic markers (Figure 5D,E), also suggested that all biofilms can maintain an undifferentiated state of hMSCs compared to our osteogenic control. We selected osteopontin (OPN), a highly abundant noncollagenous protein found in bone tissue, that has been extensively used as a marker for the early osteogenic differentiation of hMSCs<sup>[60,61]</sup> and osterix, a commonly used marker that may indicate the onset of the osteogenic differentiation of hMSCs.<sup>[62]</sup> Our data suggests an observable difference between cells cultured on all biofilms and the osteogenic control (Figure 5D), and a comparable production of OPN between the biofilm conditions and the undifferentiated hMSC control. hMSCs cultured on all biofilm conditions, except for CXCL12, showed significantly lower osterix expression than the osteogenic control (Figure 5E).

To further solidify our claim that the MSC phenotype is maintained in long term cocultures with the biofilms, we repeated the 14 d cultures and stained for the early adipogenic differentiation marker Pref-1. Consistent with our hypothesis, the expression of Pref-1 by the hMSCs was significantly downregulated

compared to the adipogenic control (Figure 5F). This trend was consistent among all biofilm conditions, with the exemption of CXCL12, where Pref-1 was expressed at statistically similar levels to the differentiated cells. The same trend was observed in cocultures of the hMSCs with combinations of the bacteria populations, in a system producing more than one recombinant protein at the same time (Figure S5A–E, Supporting Information). Having determined cell migration in a BM-resembling 3D system, we aimed to examine the effects of the same microenvironment on MSC phenotype. Therefore, we performed the same 14 d stem cell and bacteria coculture and ICW analysis in the presence of a nondegradable PEG hydrogel. Similar to the results in 2D, no loss of the naïve hMSC phenotype was observed after 14 d cultures on the biofilms, the presence of the hydrogel (Figure S5F–H, Supporting Information). Additionally, the cultured hMSCs did not show significant expression of the osteogenic markers OPN and OSX, suggesting that the addition of the 3D component in our system does not induce hMSC differentiation toward the osteogenic lineage (Figure S5I,J, Supporting Information).

Combined, our results suggest that the tested recombinant *L. lactis* biofilms can induce the maintenance of a stem-like hMSC phenotype for up to 14 d in culture, while also reducing their potential for commitment toward the osteogenic and adipogenic lineages.

## 2.6. Maintenance of the Differentiation Capacity of Human hMSCs

Having confirmed the maintenance of a naïve hMSC phenotype retained by the hMSCs after a 14 d coculture with the biofilms, we aimed to assess whether the stem cells maintain their differentiation capacity. As previously, BM human hMSCs were initially cultured on top of *L. lactis* biofilms for 14 d in hMSC maintenance media. On day 14, the maintenance medium was changed to osteogenic media, and the cells were cultured for another 14 d on the biofilms to allow differentiation. Phenotypic (ICW) analysis of the hMSCs after the 28 d showed upregulated expression of the osteogenic markers OPN and OSX, at similar levels compared to differentiated hMSCs without the presence of the biofilms (Figure 5G,H). This observation was consistent among all conditions and all bacterial populations, suggesting that the biofilms used in this work can both maintain a naïve hMSC phenotype and retain the differentiation potential of the stem cells in long term cultures.

## 3. Discussion

In the present scenario of an aging population with increased demands for injury repair and disease treatment, stem cells have been identified as a frontline regenerative medicine source. Given their therapeutic potential, recent research has focused on recreating the stem cell natural microenvironments in vitro, to drive stem cell differentiation into tissues for medical applications.

hMSCs have been the major stem cell type involved in biomedical applications due to their capacity to differentiate in

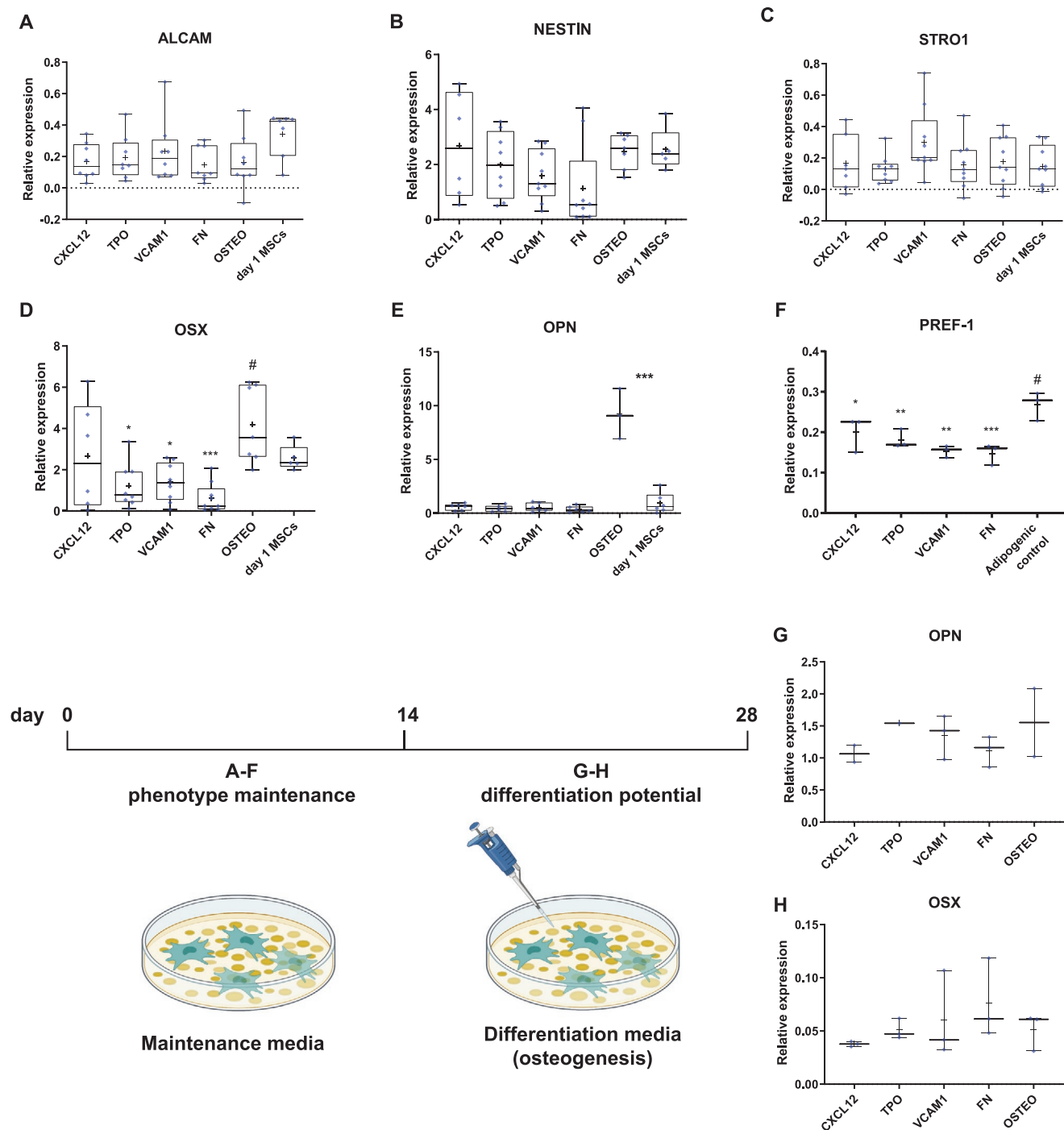


**Figure 5.** hMSC were phenotyped using in-cell Western to analyze relative expression of ALCAM, nestin, Stro1, osteopontin, and osterix. Analysis was performed after a 14 d coculture with the biofilms depicted in the graphs, namely CXCL12, TPO, VCAM1, osteogenic medium (OSTEO), and glass-only control (hMSCs). The results were normalized against beta actin and are displayed as the relative expression of each marker against the housekeeping gene. A–C) No statistical difference was observed between the stemness markers expressed by the control hMSCs and the stem cells cultured on *L. lactis*. D–E) Interestingly, increased expression of osteogenic differentiation markers osteopontin and osterix was not observed in any of the conditions except for the osteogenic medium, ( $*** p < 0.001$ ) compared to the rest of the conditions (two-way ANOVA with Tukey post hoc test) and in the OSX graph ( $* p < 0.05$ ,  $** p < 0.01$ ,  $*** p < 0.001$  compared to the reference condition, osteo, labeled as #). F) Assessment of the hMSC expression of Pref-1 after 14 d of culture also suggests that the stem cells cultured on the biofilms expressing TPO, VCAM1, and FN do not display a trend toward adipogenic differentiation. G,H) The maintenance of the differentiation potential of hMSCs cocultured with *L. lactis* was evaluated after 14 d. No statistical difference was observed between the hMSCs and osteogenic control, suggesting the maintenance of the capacity of the stem cells to differentiate after long term cultures on the biofilms. A minimum of 15 cells were measured per condition, in three independent experiments. Data presented as mean  $\pm$  SD and analyzed with ANOVA with a Tukey post hoc test. These data suggest a possible influence of the *L. lactis* biofilms in keeping an hMSC-like phenotype for up to 14 d in coculture without committing to the osteogenic lineage. SD; standard deviation.

tissues of mesodermal origin, such as chondrocytes, adipocytes, osteogenic cells<sup>[63]</sup> and neurons.<sup>[64]</sup> hMSCs reside in a variety of tissues throughout the body, and present a variety of advantageous properties for uses in regenerative medicine, such as their differentiation potential, wide availability and lack of significant histocompatibility complex expression.<sup>[65,66]</sup>

In this work we propose a system based on a bacteria-based biointerface that provides cultured hMSCs with biochemical cues present in the BM microenvironment. Our culture system is based on nonpathogenic, genetically engineered *L. lactis* NZ9020 biofilms that express human CXCL12 and TPO, as well as the signaling extracellular domain of VCAM1 and the III<sub>7-10</sub> fragment of human fibronectin. Our aim is to create a simplified in vitro BM analog that has the potential to maintain a stem-like hMSC phenotype, comparable to the naïve BM hMSCs. Our system is based on the dynamic interface between nonpathogenic *L. lactis* NZ9020 and human hMSCs, a novel culture system where the stem cells are constitutively stimulated by a variety of recombinant proteins. Our system is inspired by natural niches, where the cells are constantly receiving a variety of maintenance, expansion or differentiation signals, in comparison to most traditional cell culture methods that feature the external addition of high doses of soluble cytokines to the culture media. *L. lactis* has received the generally regarded as safe (GRAS) status by the Food and Drug Administration (FDA)<sup>[67]</sup> and has been used in a variety of clinical applications from probiotics<sup>[68]</sup> to drug delivery systems<sup>[69]</sup> and vaccination agents.<sup>[70]</sup> NZ9020 is a lactate dehydrogenase-deficient strain of *L. lactis*<sup>[71]</sup> and it is well suited for cocultures with mammalian cells, as excessive lactate production drastically reduces the pH of the culture media, making the coculture difficult. The lack of lactate dehydrogenase, plus the use of bacteriostatic antibiotics and hemin to force *L. lactis* to an aerobic metabolism gives as a result a very reduced production of lactate, keeping the pH of the culture medium close to standard cell culture values, pH 7.4.

We have selected to stimulate the cultured hMSCs with the collection of cytokines as they have been widely reported to be present in the BM and have been shown to play key roles in BM physiology and homeostasis maintenance. However, despite the wide availability of studies on the roles of soluble BM signals on other BM residing cell types, most notably hematopoietic stem cells (HSCs), not much research has been focused on the effects of these signals on hMSC fate. CXCL12 and TPO are two relevant soluble cytokines present in the BM, secreted by a variety of cells and with important roles in HSC regulation in healthy and diseased states.<sup>[72-74]</sup> VCAM1 and FN are expressed by a variety of cells in the BM and have been shown to maintain BM homeostasis and mediate hMSC and HSC function.<sup>[75-77]</sup>

Our system was optimized for long term *L. lactis* and hMSC cocultures. The use of Sigmacote as a hydrophobic coating has increased the adhesion and stability of the biofilm on the glass coverslips and has provided better surface coverage compared to other commercial silanes such as APTES. We have achieved high levels of recombinant protein production by the bacteria and have shown that the biofilm remains viable and metabolically active in our culture system.

In our coculture experiments, we have shown that the hMSCs interact with the biofilms, form focal adhesions and show an adherent, spindle-shaped appearance. In the presence

of fibronectin, both as a coating and when expressed by the biofilms, the cells obtain an elongated, spread morphotype and a significantly larger cell area compared to the rest of the culture conditions. This is a clear demonstration of the cell fate-influencing effect of the recombinant proteins on the cultured hMSCs, with a promising future potential of the system being used to further shape, direct and study hMSC fate. Furthermore, the biofilms do not show a negative impact on hMSC viability, evidence that has been consistent with previous work on *L. lactis* and mammalian cell cocultures conducted in our group.<sup>[24,25]</sup>

Furthermore, we show that hMSCs remain motile and actively explore their surrounding environment in our cocultures, with their speed and migration trajectories varying depending on the presence or absence of a 3D component (hydrogel). This 3D aspect of our system provides a higher degree of resemblance of our cultures to the BM, which is currently understood to bear mechanical and architectural properties similar to our engineered hydrogels. The higher average speeds and longer trajectories of the hMSCs cultured in the conditions featuring the degradable hydrogels further suggests that our system resembles physiological conditions, where the hMSCs would actively degrade, remodel and explore their surrounding environment.

hMSC phenotype analysis after 2 weeks of culture on different biofilms has shown that the cells maintain a naïve, stem-like phenotype, while displaying no signs of osteogenic commitment. These results were consistent in 2D cultures and in the presence of a 3D component, in the form of a hydrogel, to the system. To this date, the only studies reporting stem cell regulation by living materials have studied the potential of the biofilms to induce hMSC osteogenic differentiation. Similar to our observations, these studies have provided strong evidence that living biointerfaces can be used to direct stem cell fate. In particular, recombinant BMP-2 produced by the biofilms has been shown to induce osteogenic differentiation of hMSCs,<sup>[25]</sup> while at the same time hMSCs cultured on FN-expressing biofilms have been shown to maintain an undifferentiated phenotype and only commit to the osteogenic lineage after the addition of soluble BMP-2.<sup>[10]</sup>

In this work, we aimed to better characterize the phenotype of hMSCs cultured on the biofilms in a wider range of conditions, where the stem cells are stimulated by a range of different BM cytokines and adhesion factors. More precisely, Stro1, a marker widely used in the literature to select for hMSCs and their precursors<sup>[54,55]</sup> has been expressed in the hMSCs cultured on all biofilm conditions. Stro1 expressing cells have also been associated with migration and engraftment in a variety of tissues, as well as providing support hematopoiesis and angiogenesis.<sup>[78,79]</sup> Furthermore, high expression of Stro1 has been linked to an immature hMSC phenotype with an increased potential to proliferate and differentiate into other tissues.<sup>[58]</sup> Similarly, our biointerface has been shown to maintain nestin expression in cultured hMSCs. Nestin expression has been associated with a subset of bone marrow perivascular hMSCs which contributed to bone development, angiogenesis and are in close contact with hematopoietic stem cells (HSCs).<sup>[53]</sup> In previous research, nestin+ cells have been identified as quiescent but metabolically active and are suggested to be important

in regulating the fate of HSCs in the bone marrow.<sup>[59]</sup> Nestin-expressing hMSCs have been associated with the production of chemokine ligand 12 (CXCL12), stem cell factor (SCF), and Kit ligand (Kitl) and have been reported to be a key element of the BM niche.<sup>[53]</sup> ALCAM has also been reported in the literature as a gene expression marker for undifferentiated mesenchymal cell progenitors.<sup>[80,81]</sup> Like Stro1 and nestin, alcam has also been found expressed by the hMSCs in our cocultures, in a way statistically similar to our hMSC control.

Interestingly, all Stro1, nestin and ALCAM appear to also be preserved in the osteogenic condition. This observation is consistent with previous research, suggesting that Stro1 and alcam in particular are expressed by the fraction of the adult bone marrow hMSCs that contains the osteogenic progenitors.<sup>[82,83]</sup> Other studies have also suggested that the two markers may also be associated with the display of an osteogenic potential of hMSCs in specific cell niches.<sup>[84,85]</sup> Finally, our observation that nestin expression remains unaffected by the osteogenic conditions reported in this work is consistent with recent studies suggesting that the marker can be maintained by hMSCs in osteogenic environments.<sup>[86]</sup>

We further tested our system for expression of osteogenic markers on the cultured hMSCs. We chose OPN and OSX, two extensively used markers for the early osteogenic differentiation of hMSCs. While OPN has been identified as an early osteogenic marker,<sup>[60,61]</sup> OSX has been described as a factor widely expressed in the BM,<sup>[87]</sup> a driving force toward the osteogenic differentiation of hMSCs,<sup>[88]</sup> and an important regulator of HSC maintenance in the BM.<sup>[89]</sup> Our findings suggest that neither of the osteogenic markers described above are expressed by the hMSCs cultured on our biofilms compared to the osteogenic control. In lack of similar studies, we are the first to report that our system of hMSC-*L. lactis* cocultures has the potential to maintain the stem cells in a naïve, stem-like phenotype, while also not promoting their osteogenic differentiation. Notably, the reported maintenance of stemness was observed in hMSCs cultured on top of biofilms made up of *L. lactis* population producing a single protein and on biofilms featuring a combination of different bacterial populations (Figure S4, Supporting Information). This observation is consistent with our hypothesis that the active presentation of key BM cytokines and adhesion molecules provides a close resemblance to the signals hMSCs experience in their natural niche, contributing to the maintenance of the stem cells in a naïve, quiescent state. Therefore, we propose that our system provides a tuneable, novel representation of the hMSC niche in the BM.

Compared to previous research, these observations strengthen our hypothesis that the biointerface described here can be used as an active biomaterial for stem cell manipulation. Instead of maintaining the hMSCs in a stem-like state, the system has been previously designed to induce the osteogenic differentiation of the stem cells, after cultures on BMP-2 expressing *L. lactis* biofilms.<sup>[25]</sup> Our results and especially the stemness maintaining effect of the FN-expressing biofilms on hMSCs is also in line with previous research demonstrating that FN nanonetworks assembled on PEA are associated with enhanced, prolonged maintenance of self-renewal and retention of functional multipotency of cultured hMSCs.<sup>[90]</sup> Furthermore, in accordance with the data reported in our work, it has

been shown that the culture of hMSCs on FN-producing *L. lactis* alone is not sufficient to induce their osteogenic differentiation, which can nevertheless be achieved with external addition of soluble BMP-2.<sup>[10]</sup> This tuneable platform can therefore be easily and reproducibly tailored to each application and can shape cell fate accordingly.

## 4. Conclusion

Here, we demonstrate the potential of genetically engineered living biointerfaces to actively control stem cell behavior. Despite the number of living materials already developed, our work is based on a radical, multifaceted approach in combining the active, self-regulatory element of the biointerface, a variety of recombinant cytokines and adhesion factors produced by the bacteria and 2D and 3D culture conditions to produce novel living materials. Our approach benefits from the non-pathogenic nature of *L. lactis*, providing our system with a significant advantage over current approaches on living materials based in *E. coli*, and providing a promising potential for this work to be expanded and used in future clinical applications. We have demonstrated hMSCs can be successfully cultured on *L. lactis* biofilms, retaining high viability and displaying adhesion dynamics and cell movement comparable to traditional culture methods. Our work also provides proof that *L. lactis* can be used as a substrate to actively control hMSC behavior, retaining the cells in a naïve state in long term cultures, without affecting their differentiation potential. This new living material can be easily tuned and adjusted to a variety of applications, by instructing different recombinant protein expression or cocultures with different cell types. Our vision is that our platform will be used in further studying different aspects of stem cell fate decisions for medical applications and even in adapted versions as a clinical tool for tissue engineering applications.

## 5. Experimental Section

**Cloning:** mRNA sequences for CXCL12, TPO, and VCAM1 were retrieved from Uniprot (further details in Table S1, Supporting Information) and synthesized as dsDNA gBlocks by Integrated DNA Technologies (IDT). The synthetic sequences were subcloned in the pT2NX plasmid under the control of the strong constitutive lactococcal promoter P1,<sup>[91]</sup> flanked by the *usp45* secretion peptide to ensure extracellular secretion and, in the case of VCAM1, with the *Staphylococcus aureus* protein A fused to the C-terminus, to allow its covalent crosslinking to the peptidoglycan cell wall of *L. lactis*. A hexahistidine tag was added to each construct to allow its quantification using a competitive His-tag ELISA assay (GenScript).

Subcloning was performed using NEBuilder HiFi assembly master mix (New England Biolabs). Plasmids were transformed in electrocompetent *L. lactis*, strain NZ9020, as previously described<sup>[92]</sup> and plated in M17 agar plates supplemented with 0.5% v/v glucose and 10 µg mL<sup>-1</sup> chloramphenicol. Candidate clones were grown and sequenced to confirm the correct sequence of the inserts.

**Protein Expression Analysis:** For easier and efficient recombinant protein quantification, a 6xHis-tag had been fused to the engineered proteins expressed in *L. lactis*. For CXCL12 and TPO, bacterial supernatants were analyzed, while for VCAM1 and FN, cells were lysed using the protocol described by Cole et al.<sup>[93]</sup> Finally, the GM17C medium, used for *L. lactis* cultures, was used as a negative control. Protein expression was quantified using a competitive His-tag ELISA Detection Kit (GenScript). The

protocol includes the addition of His-tagged protein standards (11.3 kDa) ranging from 1 to 729 ng mL<sup>-1</sup> and samples to a 96-well plate precoated with a His-tagged protein, followed by the addition of an anti-His tag monoclonal antibody. The plate is then washed, and an HRP-conjugated secondary antibody is added to each well to react with anti-His tag primary antibody. Finally, 3,3',5,5'-tetramethylbenzidine (TMB) is added and after a 30 min incubation period the reaction is stopped. Sample absorbance was measured at 450 nm using a Tecan Infinite 200 microplate reader and the expression level of the His-tagged protein of interest is calculated by interpolating their OD values from the standards of the standard curve.

**Assessment of Recombinant Protein Bioactivity:** The evaluation of CXCL12 bioactivity was conducted by studying the motility dynamics of human MSCs. The stem cells were cultured overnight in sterile 24-well tissue culture plates. The following day, a 4 h culture of CXCL12-expressing *L. lactis* was conducted in DMEM, to pre-condition the media for the motility study. Following the culture, the hMSCs were incubated in DMEM conditioned with *L. lactis*-secreted or commercial CXCL12 (PeproTech), both at a concentration of 200 ng mL<sup>-1</sup>, while DMEM without any cytokine was used as a control. Stem cell motility was assessed by live phase holographic imaging, using a HoloMonitor M4 microscope (PHI). The cells were monitored for 24 h using label-free imaging and their motility was quantified by measuring the nondirectional movement and speed of the cells in our different samples. The average cell speed was automatically determined by applying the HoloMonitor Cell Motility Assay on the recorded time-lapse sequence.

To assess the biological activity of the TPO produced by *L. lactis*, the TPO-responsive human erythroleukemia TF-1 cell line (Sigma) was used.<sup>[94]</sup> Briefly, an overnight culture of TF-1 cells was incubated in RPMI media supplemented with 2 ng mL<sup>-1</sup> recombinant human granulocyte-macrophage colony-stimulating factor (GM-CSF, PeproTech) and 10% fetal bovine serum. Each sample was supplemented with 100 ng mL<sup>-1</sup> of either commercial (PeproTech) or *L. lactis*-secreted TPO using the already mentioned media conditioning protocol, and the results were compared to cells cultured in base RPMI medium without any extra GM-CSF or TPO. The cells were cultured for a total of 7 d and cell viability and number was measured on days 1, 3, 5, and 7 by pipetting a 20  $\mu$ L aliquot of cells and counting the cell density with a Countess 3 Automated Cell Counter (ThermoFisher). The TF-1 cells were seeded at an initial concentration of  $2 \times 10^5$  cells mL<sup>-1</sup>, and maintained in a humidified atmosphere incubator with 5% CO<sub>2</sub> at 37 °C.

**Glass silanization (APTES, Sigmacote):** Prior to surface preparation, 12 mm glass coverslips were sterilized by sonication in ethanol for 20 min and dried at 80 °C, followed by UV irradiation for 15 min to sterilize the surface. Then, the coverslips were dried under a dry nitrogen stream. Sterile, dried coverslips were submerged in (3-aminopropyl) triethoxysilane (APTES) or Sigmacote (Sigma) for 30 s. The silanized surfaces were then washed in ultrapure water to remove excess solution and air-dried in a laminar flow hood cabinet.

**Bacterial Culture:** *L. lactis* strain NZ9020<sup>[36]</sup> was cultured in M17 medium supplemented with 0.5% v/v sterile glucose and 5  $\mu$ g mL<sup>-1</sup> chloramphenicol. M17 is composed by tryptone (5 g L<sup>-1</sup>), soya-peptone (5 g L<sup>-1</sup>), "Lab-lemco" (5 g L<sup>-1</sup>), yeast extract (2.5 g L<sup>-1</sup>), ascorbic acid (0.5 g L<sup>-1</sup>), magnesium sulfate (250 mg L<sup>-1</sup>), and di-sodium glycerophosphate (19 g L<sup>-1</sup>) (referred as GM17C in the rest of the paper). The bacteria were grown at 30 °C in anaerobic conditions.

**Biofilm Formation and Viability:** For biofilm formation, bacterial cultures were grown overnight anaerobically as standing cultures at 30 °C in M17 medium (Formedium) supplemented with 0.5% v/v glucose and 10  $\mu$ g mL<sup>-1</sup> chloramphenicol (GM17C).

The following day, clean, sterile glass coverslips with the mentioned surface treatments (Sigmacote and APTES) and untreated glass as a control were incubated with 1 mL of fresh GM17C inoculated with 40  $\mu$ L of stationary overnight bacterial cultures. Biofilms were produced over the course of 24 h. Surfaces were washed three times with sterile ultrapure water until the planktonic bacterial phase had been removed. This resulted in a bacterial monolayer that was used for the following experiments.

Biofilm viability was assessed using the Film Tracer LIVE/DEAD Biofilm Viability Kit (ThermoFisher) after 5 and 10 d. The assay involved washing the biofilms with 0.9% NaCl solution and then incubating the biofilms in a 1:1 solution of SYTO 9:propidium iodide according to manufacturer's instructions. After a 15 min incubation, samples were imaged using a Zeiss Axio Observer epifluorescence inverted microscope. Bacterial viability was assessed by image analysis, calculating the ratio between the viable (green) and total number of bacteria (green plus red). Images were analyzed with Fiji—ImageJ software.

**Human hMSC Culture and Cell Viability:** Primary human bone-marrow derived mesenchymal stem cells (Promo cell) were maintained in DMEM supplemented with 4.5 g L<sup>-1</sup> glucose, 100  $\mu$ M sodium pyruvate,  $1 \times 10^{-3}$  M L-glutamine, 10% fetal bovine serum (FBS) and 10  $\mu$ g mL<sup>-1</sup> chloramphenicol (Cm).

To assess the viability of hMSCs cultured on the *L. lactis* biofilms, the LIVE/DEAD viability/cytotoxicity Kit (ThermoFisher) was used. Cells were washed once with PBS at 37 °C and incubated with  $2 \times 10^{-6}$  M calcein AM and  $4 \times 10^{-3}$  M ethidium homodimer in PBS. hMSCs were incubated for 30 min at room temperature protected from light and imaged with a Zeiss Axio Observer epifluorescence microscope. Viability was determined by image analysis, calculating the ratio between green (viable) and total number of cells (green plus red, nonviable cells) using Fiji-ImageJ.

**Immunostaining:** After the selected culture time, samples were fixed using 4% formaldehyde in phosphate-buffered saline (PBS) at 37 °C for 15 min. Fixative was removed and the cells were washed three times with PBS. The samples were then incubated in permeabilizing buffer (0.1% Triton X-100 in ultrapure water) for 5 min at room temperature. After a washing step, the samples were blocked with 1% BSA (bovine serum albumin) in PBS for 1 h at room temperature. A primary mouse antivinculin monoclonal antibody, hVIN1 clone (Sigma) was diluted 1:400 in 1% BSA in PBS and incubated with the samples at room temperature for 1 h. The primary antibody staining solution was removed and the samples were washed three times with PBS/Tween 20 (0.5% v/v). A Cy3-conjugated rabbit antimouse secondary antibody (Jackson ImmunoResearch) diluted 1:200 in PBS/BSA 1% was added for 1 h at room temperature in the absence of light. Samples were imaged in a fluorescence microscope (Zeiss AxioObserver Z1).

**hMSC Tracking:** Bone marrow derived hMSCs were cultured overnight on prepared *L. lactis* biofilms. Depending on the needs of each experimental setup, the hMSCs were tracked continuously for 1 or 24 h using time-lapse microscopy. During the measurements, the cells were maintained in hMSC maintenance media, at a humidified incubator at 37 °C, 5% CO<sub>2</sub>. Cell migration and average speed of displacement were measured using an EVOS FL Auto 2 microscope. Cell trajectories as position coordinates with corresponding frame numbers were saved as a Microsoft Excel file and the tracking results were analyzed using the program source codes provided by Gorelik and Gautreau.<sup>[96]</sup>

**In-Cell Western:** hMSCs were cultured on *L. lactis* biofilms for 14 d. Cells were maintained in DMEM medium supplemented with 10% FBS and an antibiotic mix consisting of 10  $\mu$ g mL<sup>-1</sup> chloramphenicol, sulfamethoxazole and tetracycline and 5  $\mu$ g mL<sup>-1</sup> hemin and erythromycin, to inhibit bacterial metabolism. For the osteogenic control,  $1 \times 10^{-6}$  M dexamethasone (D4902, Sigma), 25  $\mu$ g mL<sup>-1</sup> L-ascorbic acid (A4403, Sigma), and  $3 \times 10^{-6}$  M monobasic sodium phosphate (NaH<sub>2</sub>PO<sub>4</sub>) (S0751, Sigma) were added to hMSC base media. The adipogenic controls were cultured in base hMSC media with the addition of  $1 \times 10^{-6}$  M dexamethasone,  $500 \times 10^{-6}$  M 3-isobutyl-1-methylxanthine (IBMX) (I5879, Sigma),  $1.72 \times 10^{-6}$  M human insulin (I-034, Sigma), and  $100 \times 10^{-6}$  M indomethacin (I7378, Sigma). For the hMSC control, BM-derived hMSCs were used after one day of culture to ensure a naive phenotype.

The cocultures were incubated at 37 °C, 5% CO<sub>2</sub> in a humidified incubator with media changes every 3 d. After 14 d cells were fixed using a 4% paraformaldehyde w/v solution in phosphate-buffered saline (PBS) at 37 °C for 15 min and permeabilized using 0.1% Triton X-100 in PBS. The samples were then stained for osteopontin (OPN) (sc-21742,

Santa Cruz Biotechnology), Stro1 (sc-47733, Santa Cruz Biotechnology), nestin (sc-23927, Santa Cruz Biotechnology), osterix (OSX) (sc-393325, Santa Cruz Biotechnology) and ALCAM (CD166) (ab233750, Abcam) as well as b-actin (ab16039, Abcam) as the housekeeping protein. For detection, the IRDye 680 RD and IRDye 800 CW secondary antibodies were used for b-actin and for the rest of the aforementioned cell markers respectively (925-68071 and 926-32210, LI-COR). After the staining, the plate was dried at room temperature and read in an Odyssey Sa Infrared Imaging System (LI-COR Biosciences). Data was analyzed in ImageStudio 5.2.

**Hydrogel Formulation:** PEG hydrogels were formed using Michael-type addition reaction under physiological pH and temperature according to the protocol described by Phelps et al. (2010)30. In this work, 5% w/v polyethylene glycol-maleimide (PEGMAL) hydrogels were used, crosslinked with a 1:1 maleimide:thiol crosslinker. The crosslinkers used in this work were either PEG-dithiol (PEGSH, 2 kDa, Creative PEGWorks), or a 1:1 mixture of PEGSH and the protease-degradable peptide VPM, that is flanked by two cysteine residues (VPM peptide, GCRDVPMSMRGGDRCC, purity 96.9%, Mw 1696.96 Da, GenScript). The former composition was used for the formulation of the nondegradable hydrogels, and the latter for the degradable hydrogels. Hydrogel gelation was performed in a humidified incubator at 37 °C for 30 min. After gelation, the hydrogels were transferred on top of the hMSC-L. *lactis* cocultures.

## Supporting Information

Supporting Information is available from the Wiley Online Library or from the author.

## Acknowledgements

This work was funded by an EPSRC Program Grant (EP/P001114/1). The hMSCs used in this work were purchased from PromoCell.

## Conflict of Interest

The authors declare no conflict of interest.

## Author Contributions

The concept for this work was designed by M.J.D. and M.S.-S, while the experimental work was designed and conducted by M.P and A.R.-N. Technical advice on the synthesis of the hydrogels used in this system was provided by O.D. The results, images, and analysis were obtained and conducted by M.P and A.R.-N. The paper was written by M.P and M.S.-S.

## Data Availability Statement

The data that support the findings of this study are openly available in University of Glasgow at [https://doi.org/\[doi\], reference number 0](https://doi.org/[doi], reference number 0).

## Keywords

cell engineering, genetic engineering, living materials, microenvironment engineering, stem cells, synthetic biology

Received: March 24, 2022

Revised: May 7, 2022

Published online: May 31, 2022

- [1] A. Koyada, P. Orsu, *Regener. Eng. Transl. Med.* **2021**, *7*, 147.
- [2] A. K. Gaharwar, I. Singh, A. Khademhosseini, *Nat. Rev. Mater.* **2020**, *5*, 686.
- [3] L. A. Low, C. Mummery, B. R. Berridge, C. P. Austin, D. A. Tagle, *Nat. Rev. Drug Discovery* **2021**, *20*, 345.
- [4] E. Garreta, R. D. Kamm, S. M. Chuva de Sousa Lopes, M. A. Lancaster, R. Weiss, X. Trepal, I. Hyun, N. Montserrat, *Nat. Mater.* **2021**, *20*, 145.
- [5] P. E. Bourguine, T. Klein, A. M. Paczulla, T. Shimizu, L. Kunz, K. D. Kokkalis, D. L. Coutu, C. Lengerke, R. Skoda, T. Schroeder, I. Martin, *Proc. Natl. Acad. Sci. USA* **2018**, *115*, E5688.
- [6] M. Dominici, K. Le Blanc, I. Mueller, I. Slaper-Cortenbach, F. Marini, D. S. Krause, R. J. Deans, A. Keating, D. J. Prockop, E. M. Horwitz, *Cytotherapy* **2006**, *8*, 315.
- [7] D. Sipp, P. G. Robey, L. Turner, *Nature* **2018**, *561*, 455.
- [8] A. M. DiMarino, A. I. Caplan, T. L. Bonfield, *Front. Immunol.* **2013**, *4*, <https://doi.org/10.3389/fimmu.2013.00201>.
- [9] J. Galipeau, L. Sensébé, *Cell Stem Cell* **2018**, *22*, 824.
- [10] J. J. Hay, A. Rodrigo-Navarro, K. Hassi, V. Moulisova, M. J. Dalby, M. Salmeron-Sanchez, *Sci. Rep.* **2016**, *6*, 21809.
- [11] N. Zhu, H. Wang, B. Wang, J. Wei, W. Shan, J. Feng, H. Huang, *Stem Cells Int.* **2016**, *2016*, 5687589.
- [12] K. R. Yu, S. R. Yang, J. W. Jung, H. Kim, K. Ko, D. W. Han, S. B. Park, S. W. Choi, S. K. Kang, H. Schöler, K. S. Kang, *Stem Cells* **2012**, *30*, 876.
- [13] D. Zhang, K. A. Kilian, *Biomaterials* **2013**, *34*, 3962.
- [14] H. Gerardo, A. Lima, J. Carvalho, J. R. D. Ramos, S. Couceiro, R. D. M. Travasso, R. Pires das Neves, M. Grãos, *Sci. Rep.* **2019**, *9*, 9086.
- [15] H. I. Gungordu, M. Bao, S. van Helvert, J. A. Jansen, S. C. G. Leeuwenburgh, X. F. Walboomers, *J. Tissue Eng. Regener. Med.* **2019**, *13*, 2279.
- [16] X. Wang, T. Nakamoto, I. Dulińska, D. Dulińska-Molak, N. Kawazoe, G. Chen, *J. Mater. Chem. B* **2016**, *4*, 37.
- [17] R. J. McMurray, N. Gadegaard, P. M. Tsimbouri, K. V. Burgess, L. E. McNamara, R. Tare, K. Murawski, E. Kingham, R. O. C. C. Oreffo, M. J. Dalby, *Nat. Mater.* **2011**, *10*, 637.
- [18] M. M. Saller, W. C. Prall, D. Docheva, V. Schönitzer, T. Popov, D. Anz, H. Clausen-Schaumann, W. Mutschler, E. Volkmer, M. Schieker, H. Polzer, *Biochem. Biophys. Res. Commun.* **2012**, *423*, 379.
- [19] S. Sankaran, J. Becker, C. Wittmann, A. del Campo, *Small* **2019**, *15*, 1804717.
- [20] F. Moser, E. Tham, L. M. González, T. K. Lu, C. A. Voigt, *Adv. Funct. Mater.* **2019**, *29*, 1901788.
- [21] J. A. Getz, J. J. Rice, P. S. Daugherty, *ACS Chem. Biol.* **2011**, *6*, 837.
- [22] Z. Zhang, R. Tang, D. Zhu, W. Wang, L. Yi, L. Ma, *Sci. Rep.* **2017**, *7*, 6990.
- [23] S. Sankaran, S. Zhao, C. Muth, J. Paez, A. del Campo, *Adv. Sci.* **2018**, *5*, 1800383.
- [24] A. Rodrigo-Navarro, P. Rico, A. Saadeddin, A. J. Garcia, M. Salmeron-Sanchez, *Sci. Rep.* **2014**, *4*, 5849.
- [25] J. J. Hay, A. Rodrigo-Navarro, M. Petaroudi, A. V. Bryksin, A. J. García, T. H. Barker, M. J. Dalby, M. Salmeron-Sanchez, *Adv. Mater.* **2018**, *30*, 1804310.
- [26] T. Koivula, M. Sibakov, I. Palva, *Microbiology* **1991**, *57*, 333.
- [27] J. Borrero, J. J. Jiménez, L. Gútiérrez, C. Herranz, L. M. Cintas, P. E. Hernández, *Appl. Microbiol. Biotechnol.* **2011**, *89*, 131.
- [28] L. Steidler, J. Viaene, W. Fiers, E. Remaut, *Appl. Environ. Microbiol.* **1998**, *64*, 342.
- [29] J. M. Clements, P. Newham, M. Shepherd, R. Gilbert, T. J. Dudgeon, L. A. Needham, R. M. Edwards, L. Berry, A. Brass, M. J. Humphries, *J. Cell Sci.* **1994**, *107*, 2127.
- [30] T. A. Petrie, J. R. Capadona, C. D. Reyes, A. J. García, *Biomaterials* **2006**, *27*, 5459.

- [31] L. Liu, J. X. Chen, X. W. Zhang, Q. Sun, L. Yang, A. Liu, S. Hu, F. Guo, S. Liu, Y. Huang, Y. Yang, H. B. Qiu, *Sci. Rep.* **2018**, *8*, 204.
- [32] W. Gilbert, R. Bragg, A. M. Elmansi, M. E. McGee-Lawrence, C. M. Isales, M. W. Hamrick, W. D. Hill, S. Fulzele, *Cytokine* **2019**, *123*, 154783.
- [33] C. Hu, X. Yong, C. Li, M. Lü, D. Liu, L. Chen, J. Hu, M. Teng, D. Zhang, Y. Fan, G. Liang, *J. Surg. Res.* **2013**, *183*, 427.
- [34] S. Y. Lin, S. C. Dolfi, S. Amiri, J. Li, T. Budak-Alpdogan, K. C. Lee, C. Derenzo, D. Banerjee, J. Glod, *Int. J. Oncol.* **2013**, *43*, 1817.
- [35] H. G. Drexler, M. Zaborski, H. Quentmeier, *Leukemia* **1997**, *11*, 701.
- [36] R. S. Bongers, M. H. N. Hoefnagel, M. J. C. Starrenburg, M. A. J. Siemerink, J. G. a Arends, J. Hugenholtz, M. Kleerebezem, *J. Bacteriol.* **2003**, *185*, 4499.
- [37] E. Giaouris, M.-P. P. Chapot-Chartier, R. Briandet, *Int. J. Food Microbiol.* **2009**, *131*, 2.
- [38] S. Bayoudh, A. Othmane, L. Mora, H. Ben Ouada, *Colloids Surf., B* **2009**, *73*, 1.
- [39] F. Fathi, T. Altiraihi, S. J. Mowla, M. Movahedin, *Cytotechnology* **2009**, *59*, 11.
- [40] Z. Qian, D. Ross, W. Jia, Q. Xing, F. Zhao, *Bioact. Mater.* **2018**, *3*, 167.
- [41] I. Chopra, M. Roberts, *Microbiol. Mol. Biol. Rev.* **2001**, *65*, 232.
- [42] I. L. Huibregtse, S. A. Zaat, M. L. Kapsenberg, M. A. Sartori Da Silva, M. P. Peppelenbosch, S. J. H. Van Deventer, H. Braat, *Gastroenterol. Res. Pract.* **2012**, *2012*, 639291.
- [43] D. Pontes, S. Innocentin, S. del Carmen, J. F. Almeida, J.-G. LeBlanc, A. de Moreno de LeBlanc, S. Blugeon, C. Cherbuy, F. Lefèvre, V. Azevedo, A. Miyoshi, P. Langella, J.-M. Chatel, *PLoS One* **2012**, *7*, e44892.
- [44] A. Ya-Hsuan Ho, R. del Toro, J. Rivera-Torres, F. Louache, V. André, S. Méndez-Ferrer Correspondence, *Cell Stem Cell* **2019**, *25*, 407.
- [45] Y. Man, X. Yao, T. Yang, Y. Wang, *Front. Cell Dev. Biol.* **2021**, *9*, 14.
- [46] P. Zhang, C. Zhang, J. Li, J. Han, X. Liu, H. Yang, *Stem Cell Res. Ther.* **2019**, *10*, 327.
- [47] A. J. Engler, S. Sen, H. L. Sweeney, D. E. Discher, *Cell* **2006**, *126*, 677.
- [48] O. Dobre, M. A. G. Oliva, G. Ciccone, S. Trujillo, A. Rodrigo-Navarro, D. C. Venters, V. Llopis-Hernandez, M. Vassalli, C. Gonzalez-Garcia, M. J. Dalby, M. Salmeron-Sanchez, *Adv. Funct. Mater.* **2021**, *31*, 2170150.
- [49] G. A. Foster, D. M. Headen, C. González-García, M. Salmerón-Sánchez, H. Shirwan, A. J. García, *Biomaterials* **2017**, *113*, 170.
- [50] J. Patterson, J. A. Hubbell, *Biomaterials* **2010**, *31*, 7836.
- [51] R. Zohar, S. Cheifetz, C. A. G. McCulloch, J. Sodek, *Eur. J. Oral Sci.* **1998**, *106*, 401.
- [52] J.-W. Choi, S. Shin, C. Y. Lee, J. Lee, H.-H. Seo, S. Lim, S. Lee, I.-K. Kim, H.-B. Lee, S. W. Kim, K.-C. Hwang, *Cell. Physiol. Biochem.* **2017**, *44*, 53.
- [53] L. Xie, X. Zeng, J. Hu, Q. Chen, *Stem Cells Int.* **2015**, *2015*, <https://doi.org/10.1155/2015/762098>.
- [54] S. Gronthos, A. C. W. Zannettino, S. J. Hay, S. Shi, S. E. Graves, A. Kortesidis, P. J. Simmons, *J. Cell Sci.* **2003**, *116*, 1827.
- [55] P. Simmons, B. Torok-Storb, *Blood* **1991**, *78*.
- [56] F. Arai, O. Ohneda, T. Miyamoto, X. Q. Zhang, T. Suda, *J. Exp. Med.* **2002**, *195*, 1549.
- [57] J. Lin, C. Redies, *Dev. Genes Evol.* **2012**, *222*, 369.
- [58] J. E. Dennis, J.-P. Carbillet, A. I. Caplan, P. Charbord, *Cells Tissues Organs* **2002**, *170*, 73.
- [59] S. Méndez-Ferrer, T. V. Michurina, F. Ferraro, A. R. Mazloom, B. D. MacArthur, S. A. Lira, D. T. Scadden, A. Ma'ayan, G. N. Enikolopov, P. S. Frenette, *Nature* **2010**, *466*, 829.
- [60] J. E. Aubin, *Rev. Endocr. Metab. Disord.* **2001**, *2*, 81.
- [61] D. J. Rickard, T. A. Sullivan, B. J. Shenker, P. S. Leboy, I. Kazhdan, *Dev. Biol.* **1994**, *161*, 218.
- [62] F. P. Barry, J. M. Murphy, *Int. J. Biochem. Cell Biol.* **2004**, *36*, 568.
- [63] H. E. Owston, P. Ganguly, G. Tronci, S. J. Russell, P. V. Giannoudis, E. A. Jones, *Stem Cells Int.* **2019**, *2019*, <https://doi.org/10.1155/2019/6074245>.
- [64] D. N. Urrutia, P. Caviedes, R. Mardones, J. J. Minguell, A. M. Vega-Letter, C. M. Jofre, *PLoS One* **2019**, *14*, e0213032.
- [65] C. Campagnoli, I. A. G. Roberts, S. Kumar, P. R. Bennett, I. Bellantuono, N. M. Fisk, *Blood* **2001**, *98*, 2396.
- [66] C. de Vasconcellos Machado, P. D. da Silva Telles, I. L. O. Nascimento, *Rev. Bras. Hematol. Hemoter.* **2013**, *35*, 62.
- [67] S. Wessels, L. Axelsson, E. Bech Hansen, L. De Vuyst, S. Laulund, L. Lähteenmäki, S. Lindgren, B. Mollet, S. Salminen, A. Von Wright, *Trends Food Sci. Technol.* **2004**, *15*, 498.
- [68] M. Liu, X. Zhang, Y. Hao, J. Ding, J. Shen, Z. Xue, W. Qi, Z. Li, Y. Song, T. Zhang, N. Wang, *Food Funct.* **2019**, *10*, 1132.
- [69] M. Medina, E. Vintiñi, J. Villena, R. Raya, S. Alvarez, *Bioeng. Bugs* **2010**, *1*, 313.
- [70] M. Azizpour, S. D. Hosseini, P. Jafari, N. Akbary, *Avicenna J. Med. Biotechnol.* **2017**, *9*, 163.
- [71] M. Kaur, G. Jayaraman, *Metab. Eng. Commun.* **2016**, *3*, 15.
- [72] T. Nagasawa, in *The Chemokine CXCL12 and Regulation of Hsc and B Lymphocyte Development in the Bone Marrow Niche*, Vol. 602, Springer, Boston, MA **2007**, pp. 69–75.
- [73] P. Agarwal, H. Li, A. J. Paterson, J. He, T. Nagasawa, R. Bhatia, *Blood* **2016**, *128*, 26.
- [74] A. P. Ng, M. Kauppi, D. Metcalf, L. Di Rago, C. D. Hyland, W. S. Alexander, *Proc. Natl. Acad. Sci. USA* **2012**, *109*, 2364.
- [75] T. Ulyanova, L. M. Scott, G. V. Priestley, Y. Jiang, B. Nakamoto, P. A. Koni, T. Papayannopoulou, *Blood* **2005**, *106*, 86.
- [76] S. Lu, M. Ge, Y. Zheng, J. Li, X. Feng, S. Feng, J. Huang, Y. Feng, D. Yang, J. Shi, F. Chen, Z. Han, *Stem Cell Res. Ther.* **2017**, *8*, 178.
- [77] J. S. Choi, B. A. C. Harley, *Sci. Adv.* **2017**, *3*, <https://doi.org/10.1126/sciadv.1600455>.
- [78] R. Gonçalves, C. Lobato da Silva, J. M. S. Cabral, E. D. Zanjani, G. Almeida-Porada, *Exp. Hematol.* **2006**, *34*, 1353.
- [79] M. Bentsidhoum, A. Chapel, S. Francois, C. Demarquay, C. Mazurier, L. Fouillard, S. Bouchet, J. M. Bertho, P. Gourmelon, J. Aigueperse, P. Charbord, N. C. Gorin, D. Thierry, M. Lopez, *Blood* **2004**, *103*, 3313.
- [80] X. Hu, M. Garcia, L. Weng, X. Jung, J. L. Murakami, B. Kumar, C. D. Warden, I. Todorov, C. C. Chen, *Nat. Commun.* **2016**, *7*, 13095.
- [81] B. Brinkhof, B. Zhang, Z. Cui, H. Ye, H. Wang, *Gene X* **2020**, *5*, 100031.
- [82] R. A. Hooker, B. R. Chitteti, P. H. Egan, Y. H. Cheng, E. R. Himes, T. Meijome, E. F. Srour, R. K. Fuchs, M. A. Kacena, *J. Musculoskeletal Neuronal Interact.* **2015**, *15*, 83.
- [83] S. Gronthos, S. E. Graves, S. Ohta, P. J. Simmons, *Blood* **1994**, *84*, 4164.
- [84] P. Ercal, G. G. Pekozer, O. Z. Gumru, G. T. Kose, M. Ramazanoglu, *Arch. Oral Biol.* **2017**, *82*, 293.
- [85] S. P. Bruder, N. S. Ricalton, R. E. Boynton, T. J. Connolly, N. Jaiswal, J. Zaia, F. P. Barry, *J. Bone Miner. Res.* **1998**, *13*, 655.
- [86] A. Wong, E. Ghassemi, C. E. Yellowley, *BMC Vet. Res.* **2014**, *10*, 173.
- [87] M. Seike, Y. Omatsu, H. Watanabe, G. Kondoh, T. Nagasawa, *Genes Dev.* **2018**, *32*, 359.
- [88] M. Fakhry, E. Hamade, B. Badran, R. Buchet, D. Magne, *World J. Stem Cells* **2013**, *5*, 136.
- [89] T. Mizoguchi, S. Pinho, J. Ahmed, Y. Kunisaki, M. Hanoun, A. Mendelson, N. Ono, H. M. Kronenberg, P. S. Frenette, D. S. Gottsman, *Dev. Cell* **2014**, *29*, 340.
- [90] P. Rico, H. Mnatsakanyan, M. J. Dalby, M. Salmerón-Sánchez, *Adv. Funct. Mater.* **2016**, *26*, 6563.
- [91] L. Schotte, L. Steidler, J. Vandekerckhove, E. Remaut, *Enzyme Microb. Technol.* **2000**, *27*, 761.
- [92] H. Holo, I. F. Nes, *Appl. Environ. Microbiol.* **1989**, *55*, 3119.
- [93] J. N. Cole, S. P. Djordjevic, M. J. Walker, in *Isolation and Solubilization of Gram-Positive Bacterial Cell Wall-Associated Proteins*, Vol. 425, **2008**, pp. 295–311.
- [94] H. Drexler, M. Zaborski, H. Quentmeier, *Leukemia* **1997**, *11*, 701.
- [95] R. Gorelik, A. Gautreau, *Nat. Protoc.* **2014**, *9*, 1931.